Bioorthogonal Reactions in Animals

Karine Porte, Maxime Riberaud, Rémi Châtre, Davide Audisio, Sébastien Papot, Frédéric Taran

Bioorthogonal reactions in animals

Karine Porte,[a] + Maxime Riberaud,[a] + Rémi Châtre,[b] Davide Audisio,[a] Sébastien Papot*[b] and Frédéric Taran*[a]

Abstract: The advent of bioorthogonal chemistry has enabled the development of powerful chemical tools allowing to envision increasingly ambitious applications. In particular, these tools have made it possible to achieve what is probably the holy grail for many researchers involved in chemical biology: to perform non-natural chemical reactions within living organisms. In this minireview, we present an update of bioorthogonal reactions that have been carried out in animals for various applications. We outline the advances made in both understanding biological processes and developing innovative imaging and therapeutic strategies by using bioorthogonal chemistry.

1. Introduction

In 2003, Bertozzi and co-workers introduced for the first time the concept of bioorthogonal chemistry.[1] Since then, the interest in this kind of chemistry has continued to grow exponentially and has become an essential tool in chemical biology.[2] Initially developed to understand and modulate biological fundamental mechanisms, bioorthogonal chemistry has recently found potential applications in the fields of diagnosis and targeted therapies. A rapid survey of the literature clearly indicates a dramatic increase in the number of publications over the last 10 years dealing with biorthogonal reactions on and inside living cells but chemistry within living animals, that is more complex to carry out, remains by far less explored. Several excellent perspective reviews have already treated some aspects of the emerging applications of *in vivo* chemistry.[3] Herein, we present an update of the recent examples of biorthogonal chemistry accomplished in animals to understand biological processes as well as to develop innovative diagnosis or therapeutic tools.

By definition, bioorthogonal reactions are compatible with biological media, display incredible selectivity and ideally involve stable, inert, non-natural chemical functions. However, these parameters alone are not sufficient for successful *in vivo* chemistry. Biostability, non-toxicity, favourable pharmacokinetics of bioorthogonal reactants and high kinetics of the reaction are also mandatory prerequisites. However, despite the importance of these parameters, only few studies have been performed to demonstrate the real *in vivo* bioorthogonality of the reactions and the biostability of the reactants.[4] Bioorthogonal reactions can be classified in three main categories: ligation,[5] cleavage[6] and click-and-release reactions.[7] Among the ligation reactions that have found a wide scope of *in vivo* applications (Figure 1a), the Tetrazine (Tz)/Trans-cyclooctene (TCO) ligation is the most described in the literature as the consequence of its favourable kinetics providing the most significant *in vivo* results. Furthermore, the Strain-promoted Azide-Alkyne (SPAAC) and Sydnone-Alkyne (SPSAC) cycloaddition reactions have also been successfully investigated for *in vivo* applications. Click and release reactions offer the possibility not only to link two molecules together but also to release a compound of interest, providing many new perspectives. Nowadays, only three click-and-release reactions have been successfully used in animals.

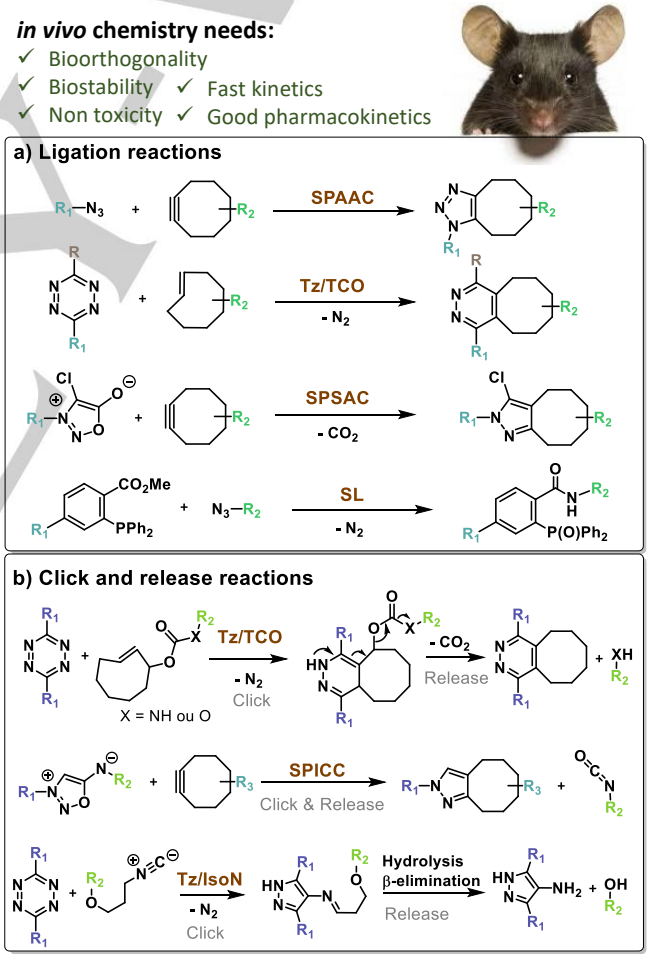

Figure 1. Main bioorthogonal reactions used for *in vivo* applications.

The most widely used reaction is the one involving Tz and TCO derivatized by a carbamate adjacent to the olefin. Described for the first time by M. Robillard and co-workers in 2013 (Figure 1b),[8] this reaction has been recently improved in order to combine high kinetics and yields of released molecules.[9] The second reaction, which has been described in 2017 by our team,

[a] Dr. Karine Porte, M. Riberaud, Dr. D. Audisio and Dr. F. Taran
Université Paris-Saclay, CEA, INRAE, Département Médicaments et Technologies pour la Santé (DMTS), SCBM, 91191 Gif-sur-Yvette, France.
E-mail: frederic.taran@cea.fr
+ These authors contributed equally to this review.
[b] Pr. S. Papot, R. Châtre
Université de Poitiers, UMR-CNRS 7285, Institut de Chimie des Milieux et des Matériaux de Poitiers (IC2MP), F-86022, Poitiers, France
E-mail : sebastien.papot@univ-poitiers.fr

correspond to [3+2] cycloaddition followed by a retro Diels-Alder between Iminosydnones and Cyclooctynes (Strain-Promoted Iminosydnone-Cycloalkyne Cycloaddition, SPICC).[10] Very recently, Franzini *et al.* showed the applicability of the reaction between tetrazines (Tz) and isonitriles (IsoN) for the decaging of drugs. The reaction yields 4-iminopyrazoles, which upon hydrolysis and subsequent β-elimination successfully release fluorophores or active drugs in zebrafish embryos.[11]

2. *In vivo* chemistry to study fundamental biological mechanisms

2.1 Glycome imaging in zebrafish and mice

After their pioneer work on Staudinger ligation (SL)[12],[13] and copper-catalyzed click chemistry[14],[15] to detect azide-labeled biomolecules on cells, Bertozzi and co-workers made the first step toward the use of bioorthogonal reactions in living systems. They brilliantly demonstrated that this chemistry can be a powerful tool to understand fundamental living mechanisms. By using an unnatural sugar containing an azide moiety, they developed an imaging method of glycans in zebrafish embryos.[16] After metabolic incorporation of peracetylated *N*-azidoacetylgalactosamine ($Ac_4GalNAz$), addition of DIFO probes allowed the imaging of glycans into zebrafish embryos *via* SPAAC (Figure 2).

Using this methodology, the same group was also able to study the dynamic behaviour of glycans during zebrafish development by using up to three different dyes over time. This robust approach of metabolic labeling with $Ac_4GalNAz$ followed by detection *via* SPAAC, revealed differences in the cell-surface expression, but also in tissue distribution of glycans during zebrafish embryogenesis.

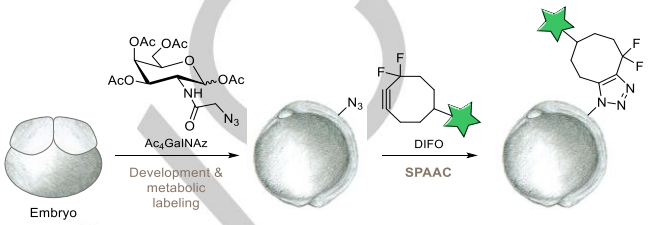

Figure 2. Schematic representation of cell-surface glycans imaging during zebrafish development.

Few years later, Wu and co-workers, reported the use of CuAAC ligation reaction for imaging of fucosylated glycans during zebrafish early embryogenesis.[17] However, while this metal-

Karine Porte joined the group of Dr. Taran for her PhD degree in chemistry at the Atomic Energy and alternative Energy Commission (CEA) in 2016. Her PhD research was focus on the use of bioorthogonal chemistry for drug delivery. After obtaining her PhD in September 2019, she moved to a postdoctoral position in the group of Prof. Frank Glorius at the University of Münster.

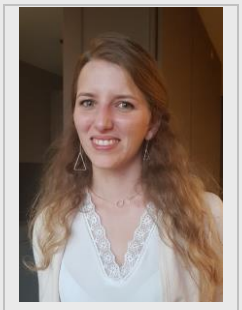

Davide Audisio holds a PhD from the University Paris-Sud. After a postdoctoral experience at the Max-Planck-Institut für Kohlenforschung (Germany), in 2012 he joined the chemistry department of Eli Lilly & Co (UK). Next, he joined the CEA and since 2016, he is in charge of the Laboratory of Carbon-14 Labeling. In 2019, he was recipient of an ERC Consolidator Grant devoted to the development of late-stage radiocarbon labeling.

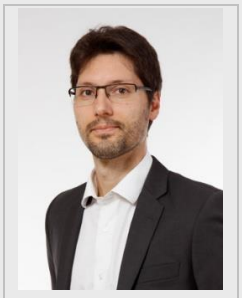

Maxime Ribéraud received his master degree from Poitiers University in 2019 and he is currently working toward his PhD degree in organic chemistry at the Atomic Energy and alternative Energy Commission (CEA). His current research focuses on developing new methodes for the detection and the quantification of tumor receptors by bioorthogonal chemistry.

Sébastien Papot is Professor of organic chemistry at the University of Poitiers (France) where he is heading the Programmed Molecular Systems Team within the IC2MP (Institut de Chimie des Milieux et des Matériaux de Poitiers). His research interests include the design of smart drug delivery systems for cancer chemotherapy, *in vivo* chemistry, functional interlocked systems and prebiotic chemistry.

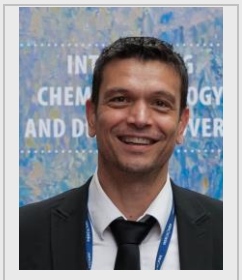

Rémi Châtre works toward obtaining his PhD degree at the Institut de Chimie des Milieux et Matériaux de Poitiers (IC2MP). His PhD research focused in the development of bioorthogonal approaches for modifying serum albumin *in vivo* to improve therapeutic efficacy of albumin drug conjugates..

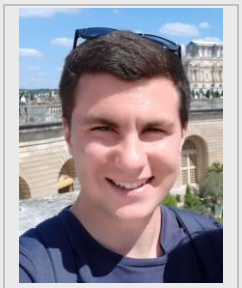

Dr. Taran secured a PhD in chemistry at the Paris XI University under the supervision of Dr. Charles Mioskowski and then moved to a post-doctoral position with Prof. Sir Derek Barton at Texas A&M University. Since 1998, he works for the French Alternative Energies and Atomic Energy Commission (CEA) located at Saclay, close to Paris and is now in charge of the department of bioorganic chemistry.

catalysed strategy permitted efficient glycans labelling in zebrafish,[18],[19] its transfer in more complex living systems such as mice remains problematic. Indeed, in the case of this three components-based reaction, the azide, alkyne and copper catalyst have to be targeted in the same tissue to reach efficient concentrations, which is highly challenging. Furthermore, the potential toxicity of the copper is still an issue for the exploitation of this bioorthogonal reaction in mammals. In 2010, Bertozzi and co-workers demonstrated that the bioorthogonal ligation reaction between cyclooctynes and azides can occur under the physiological conditions prevailing in living mice.[20] First, the mice were injected with Ac_4ManNAz once a day for one week to metabolically incorporate azides to cell-surface sialoglycoconjugates (Figure 3). After metabolic labelling, the corresponding azido sialic acids (SiaNAz) reacted *in vivo* through SPAAC reaction with a panel of cyclooctynes functionalized with a water-soluble FLAG peptide epitope tag (DYKDDDDK) to facilitate the detection of the ligation products. Finally, mice were euthanized and the splenocytes isolated to study the presence of cycloadducts by flow cytometry analysis. These experiments demonstrated that the biorthogonal reaction occurred *in vivo* at the surface of cells with an efficacy that was dependent of the structure of the cyclooctyne conjugate.

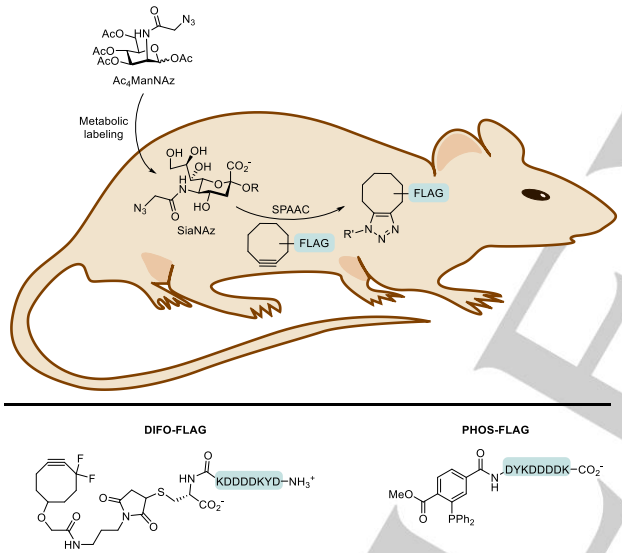

Figure 3. Schematic representation of the chemistry in mice. Mice were injected with Ac_4ManNAz to allow metabolic labeling of glycans with SiaNAz. The injection of a cyclooctyne-FLAG conjugate induce the *in vivo* covalent labeling of azido glycans. Structure of DIFO-FLAG for SPAAC reaction and PHOS-FLAG for Staudinger ligation.

The obtained outcomes showed that in addition to the intrinsic reactivity of bioorthogonal reagents, their pharmacokinetics played also a crucial role for cell labelling *in vivo*. Indeed, DIFO-FLAG which possesses the best reactivity with azides *in vitro* was less efficient than PHOS-FLAG, a reagent with a lower inherent reactivity with azides (Staudinger ligation), for the bioorthogonal labelling of splenocytes *in vivo.*

2.2 *In vivo* click to image the microbiota

In 2015, Kasper and co-workers, employed for the first time bioorthogonal reaction for *in vivo* imaging and tracking of host–microbiota interactions *via* metabolic labelling **of** gut anaerobic bacteria.[21] In this study, the authors used DIBO derivatives to track living bacteria. In a first instance, they incorporated azide functional groups into polysaccharides of *B. fragilis* by supplementing bacterial growth medium with azide-modified tetraacetylated-N-azidoacetylgalactosamine (GalNAz, Figure 4a). The subsequent incubation of cyclooctyne derivatives into the culture medium allowed the fluorescent labelling of *B. fragilis* by copper-free click reaction.

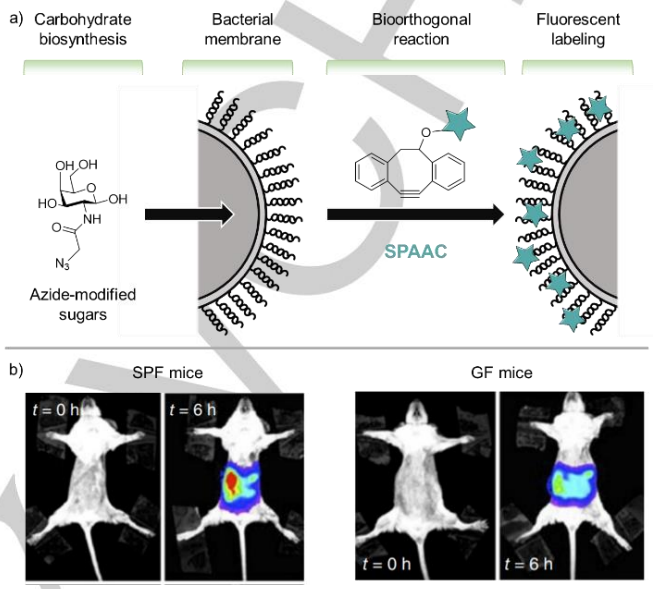

Figure 4. a) Schematic representation of bacteria labeling by copper-free click chemistry. b) *In vivo* visualization of *B. fragilis* in the instestine. Whole body imaging by IVIS of Cy7-labeled *B. fragilis* in conventional specific-pathogen-free (SPF) and germ free (GF) mice.

After this first proof of concept, this strategy was adapted to visualize in real-time bacteria dissemination along the intestine in live mice (Figure 4b). Thus, by combining metabolic oligosaccharide engineering and bioorthogonal click chemistry, the authors reported an efficient method to detect and track live *B. fragilis* in the host.

2.3 *In vivo* enzyme profiling

Recently, bioorthogonal reactions emerged as efficient tools for profiling the activity of enzymes *in vivo* and understanding the role of these proteins in physiological and pathological processes. Dubikovskaya and co-workers described *in vivo* ligation between D-cysteine (D-Cys) and 2-cyanobenzothiazoles (CBT) to generate D-luciferin substrates for bioluminescent imaging of protease activity in living mice.[22] The authors tested this approach for a real time imaging of apoptosis associated with caspase 3/7 activities in living mice. The activity of caspase 3/7 was induced in the mice by injection of lipopolysaccharide (LPS) and D-galactosamine (d-GalN). Then, a combination of CBT and protected peptide substrate Asp-Glu-Val-Asp-D-Cys (DEVD-(D-Cys)) were injected to the mice (Figure 5). The caspase 3/7 activity in mice triggered the release of free D-Cys which upon bioorthogonal reaction with CBT allowed the formation of luciferin substrates with subsequent light emission from luciferase. The light was detected using a charge-coupled device (CCD) camera. In these experiments, the controlled caspase 3/7-catalysed luciferin formation produced a better light signal than that obtained using commercially available DEVD-aminoluciferin substrate,

therefore showing the potential of this approach for both the quantification and imaging of protease activities in living animals.

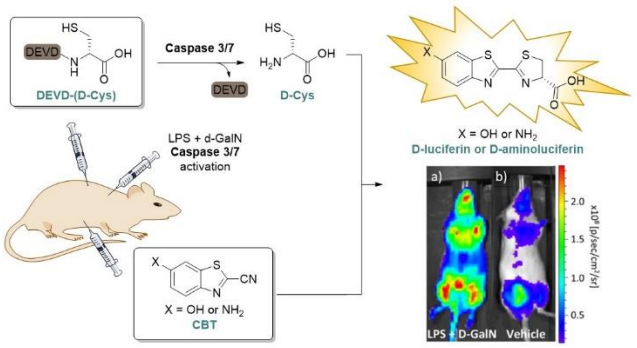

Figure 5. Formation of luciferin substrates *in vivo* by selective reactions of cyanobenzothiazoles (CBT) with D-Cysteine. Imaging of enzymatic activity in mice by D-aminoluciferin formation *in vivo* with (a) or without (b) caspase 3/7 activation.

3 *In vivo* imaging for diagnostic purposes

3.1 Pretargeting strategies

During the past 30 years, numerous pretargeting methods have been developed, with several preclinical results for both radiotherapy and radioimaging purposes. Pretargeting is a two steps strategy, which consist in (1) administering modified antibodies (mAbs) that can bind a specific biological target, and (2) injecting a radiolabelled probe that can react with the mAbs-target complex (Figure 6).

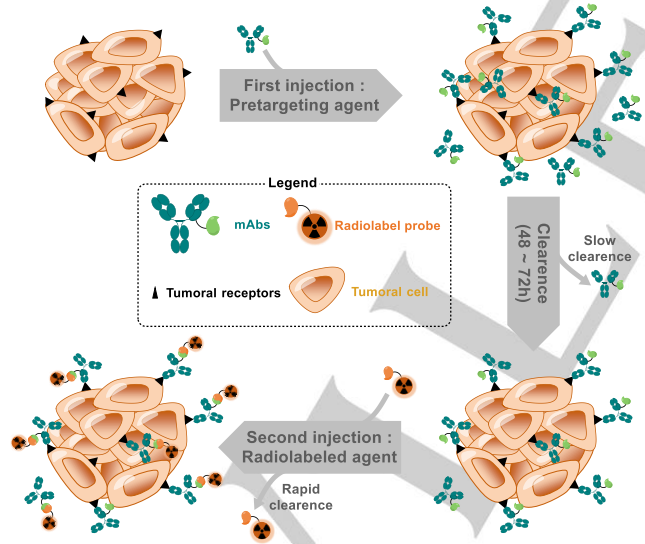

Figure 6. Schematic representation of the mostly use pretargeting strategy for radioimagery or radiotherapy using bioorthogonal functions.

The first pretargeting approach was described at the end of the 80's by Hnatowich *et al*.[23]. They used the biotin-streptavidin interaction to target agarose-streptavidin beads with ^{111}In-Biotin in living mice. However, this strategy was abandoned in phase II due to the streptavidin toxicity induced by the non-specific binding to endogenous biotin.

In 2011, van Dongen and co-workers[24] were the first to attempt a bioorthogonal approach for tumour pretargeting in living mice using the Staudinger ligation (SL) reaction. However, results did not live up to expectations probably due to the slow kinetics of the ligation reaction.

A few years later, the groups of Kim and Lee proposed to employ the SPAAC reaction instead of SL in order to improve the kinetics of the ligation.[25] For this purpose, they prepared glycol chitosan nanoparticles containing azides which they radiolabelled *in vivo* with ^{64}Cu-DOTA-Lys-PEG$_4$-DBCO for PET imaging. With this approach, they were able to localize tumours in mice bearing SCC7 xenografts.

In 2013, Robillard and co-workers synthetized anti-CD20 mAbs functionalized with azides and a series of ^{177}Lu-labelled DOTA linked to cyclooctyne derivatives with the aim to evaluate their capability to react in mice.[26] Unfortunately, control experiments carried out in mice without tumours highlighted the low efficiency of the SPAAC reaction. Shortly afterward, Kim and co-workers also used the SPAAC reaction to develop a pretargeting approach based on the permeability and retention effect (EPR) with mesoporous silica nanoparticles as the targeting unit instead of mAbs.[27] These nanoparticles were previously functionalized by dibenzocyclooctyne (DBCO) and administered into tumour-bearing mice. Once non-targeted nanoparticles eliminated from the blood (24 h after their *i.v.* administration), a ^{18}F-labelled azide was injected and the accumulation of radioactivity was followed by PET-CT imaging. Under these conditions, an accumulation of the radioactivity at the tumour site was observed while much less radioactivity was detected in the control group that did not received the pretargeting agent. These results indicated that SPAAC can be successfully used for tumour pretargeting but preferentially using nanoparticles with high density of biorthogonal functions at their surfaces.

Undoubtedly, the most efficient reaction for pretargeting is the inverse-electron-demand Diels–Alder reaction (IEDDA) reaction between *trans*-cyclooctene (TCO) and tetrazine derivatives (Tz). The first use of TCO/Tz reaction for pretargeting application in living mice was described in 2010 by Rossin *et al.* (Figure 7, entry 1).[28] They injected a non-internalizing CC49 mAbs functionalized with PEG$_{12}$-TCO moieties to mice-bearing colorectal tumors (LS174T). After a clearance time of 24 hours, a radiolabeled-^{111}In-DOTA-PEG$_{12}$-Tz was then administered. Radioactivity monitoring by SPECT-CT proved the efficacy of IEDDA reaction for pretargeting purposes. Furthermore, pioneer work from Weissleder in 2012 demonstrated the importance of the clearance kinetics of the radiolabeled secondary agent.[29] Their work indicated indeed that long circulating derivatives such as polymers might strongly increase the *in vivo* labelling efficiency.

Several other experiments were conducted by many teams using different tumour models, mAbs-TCO, Tz-based radioligands and different radioisotopes (^{111}In, ^{18}F, ^{99m}TC, ^{64}Cu, ^{212}Pb ^{177}Lu, ^{225}Ac, ^{68}Ga). In Figure 7 we selected some of the successive improvements in the pretargeting strategies developed for imaging purposes.[30]

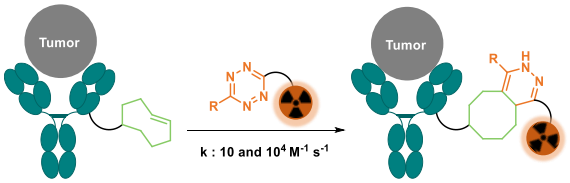

Entry	mAbs	Radiolabel	Tumor model	Imagery	Ref.
1	CC49-PEG$_{12}$-TCO	Tz-PEG$_{11}$-DOTA-^{111}In	LS174T	SPECT	28
2[a]	CC49-TCO	Tz-PEG$_{11}$-DOTA-^{111}In	LS174T	SPECT	31
3	5B1-TCO	Tz-PEG$_{11}$-Al-NOTA-^{18}F	BxPC3	PET	30a
4[a]	5B1-DFO-TCO	Tz-PEG$_{11}$-NOTA-^{68}Ga	BxPC3	PET	35
5	Anti-CD45-TCO	Tz-PMT10-^{18}F	LS174T	PET	29
6	35A7-PEG$_{0,4,12}$-TCO	Tz-Cy5	A431-CEA-Luc	NIRF	30b
7	CC49-PEG$_{12}$-TCO	Tz-PEG$_{11}$-DOTA-^{111}In	LS174T	Ultrasound	38

[a] Clearing agents were used

Figure 7. Highlighted *in vivo* pretargeting studies involving TCO/Tz approach.

An issue that arises with pretargeting strategies is that a significant portion of the injected antibody remains in circulation, causing a reduction in target-to-background ratios. In 2013 Robillard *et al.* used for the first time a masking TCO agent to neutralize circulating antibodies in order to improve the pretargeting approach (Figure 7, entry 2).[31] The idea was to inject a clearing Tz-based reagent, which can specifically react with the free circulating TCO-mAbs in the blood stream (and not at the tumor site), in order to mask these mAbs before the injection of the Tz-based radioligand. They demonstrated the value of this concept with a Tz-based-galactose clearing agent (CA) which allowed an improvement of 125-fold of the tumour/blood ratio. Following these results, several other teams tried to improve CAs by using different clearing moiety such as albumin, polystyrene-based particles, or dextran polymers. [32],[32],[33],[34],[35],[36]

IEDDA-based pretargeting approach was implemented by Lin's team with the use of TCO-functionalised nanoparticles.[37] They first administrated the nanoparticles into mice with tumours and, after a delay of 24h, injected a ^{64}Cu-radiolabelled Tz-DOTA complex and followed the reaction by PET imaging. They found a strong PET signal at the tumour site, but also in the liver due to trapping of the nanoparticles by the mononuclear phagocyte system or trans-chelation of ^{64}Cu from DOTA *in vivo*.

In addition to the radiodetection or NIR detection, Valliant and co-workers extended the TCO/Tz pretargeting approach to ultrasound imaging (Figure 7, entry 7).[38] They first injected TCO-conjugated mAbs VEGFR2-positive (modified EGFR antigen) murine xenografts and after 24 hours of clearance delay, they administered intravenously Tz-functionalized microbubbles and monitored the reaction by ultrasound imaging. They demonstrate high retention of the microbubbles at the tumour site with significant contrast enhancement compared to mice without TCO–mAb pre-treatment.

Despite all these encouraging results, pretargeting approaches based on the TCO/Tz reaction has not reached clinical trials yet. The main problem remains the TCO isomerization into its inactive form (*cis*-cyclooctene) that cannot react with the tetrazine moiety. Nevertheless, some teams tried to minimize these side reactions by modulating some parameters of the mAbs such as the PEG linker length, the number of TCO per antibody and their localisation on the immunoconjugate. The Tz structure was also tuned to improve pharmacokinetics. For more details on the recent advancements up to the year 2019 on the TCO/Tz pretargeting approach, we direct the readers to consult the recent review published by Rondon and Degoul.[39]

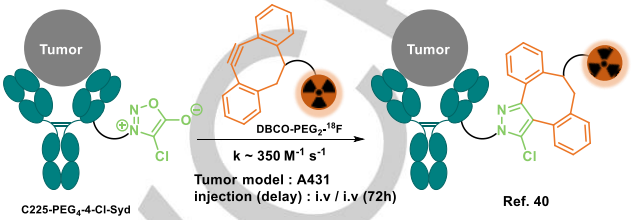

Figure 8. *in vivo* pretargeting studies involving SPSAC approach

Besides the above-described reactions, our team recently evaluated the SPSAC reaction for *in vivo* PET imaging (Figure 8).[40] We demonstrated that this strain promoted reaction between 4-chloro-sydnones and [^{18}F]F-PEG$_2$-DBCO can occur *in vivo* with a good kinetic (k = 300 L mol^{-1} s^{-1}). PET imaging of mice bearing subcutaneous A431 xenografts showed a specific tumour uptake but hepatobiliary elimination of the [^{18}F]F-PEG$_2$-DBCO was very low, leading to a low imaging contrast. With further optimization of the labelled cyclooctyne pharmacokinetics, we do hope that this strategy becomes a practical tool for pretargeting imaging.

3.2 Cancer imaging using metabolic glycoengineering

Among the chemical biology approaches to study cancers, metabolic glycoengineering (MGE) is one of the most used alternatives to the classic pretargeting. Specific changes in glycan profiles, such as overexpression of sialic acid in tumour tissues suggest that glycans could be employed in clinical diagnostics.[41] MGE involves the introduction of non-natural chemical groups into the surface of cells by metabolization of specific monosaccharides bearing a bioorthogonal functional group. Among them, the azide moiety is the most utilized because its incorporation into the tumour glycan is well established through metabolization of the monosaccharide Ac$_4$ManNAz. Cancer cells decorated by multiple azide functions can then be functionalized and detected through either the SPAAC or SL reactions.

Brindle and co-workers brilliantly demonstrated for the first time an *in vivo* bioorthogonal metabolic labelling strategy allowing the detection of sialylated cell surface glycans by radio- and fluorescence imaging (Figure 9, entry 1).[42] They intraperitoneally injected Ac$_4$ManNAz, which was metabolized in azidosialic acid and incorporated at the surface of cancer cells. After 24h, they injected a biotinylated phosphine (bPhp) which can react by SL with the azidosialic acids present at the surface of tumour cells. Finally, the biotin moiety was detected by subsequent intravenous injection of a fluorescent or radiolabeled avidin derivative. Because SL and SPAAC reactions are rather slow, targeting strategies to increase the local concentrations of either the phosphine or cyclooctyne partners might improve the efficiency of the attachment to the azides incorporated into tumor glycans. Koo and co-workers[43] were the first to follow this strategy by

introducing azide groups into tumor-A549-bearing mice through intra-tumoral injection of $Ac_4ManNAz$ followed by *i.v* administration of DBCO encapsulated in liposomes (Figure 9, entry 2).

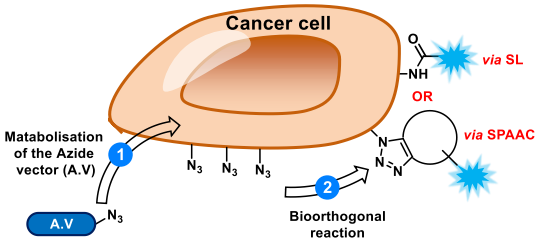

Entry	Azide vector	Bioorthogonal reaction	Targeting agent	Tumor model	Ref.
1	$Ac_4ManNAz$	SL	bPhp	LL/2	42
2	$Ac_4ManNAz$	SPAAC	DBCO-liposome	A549	43
3	$Ac_4ManNAz$ -CNPs	SPAAC	BCN-Ce6-CNPs	A549	47
4	$Ac_4ManNAz$ -microbubble	SPAAC	DBCO-Cy5	41T	48
5	RR-S-$Ac_3ManNAz$	SPAAC	DBCO-Cy5.5	HT-29	45
6	$Ac_4ManNAz$ -liposome	SPAAC	DBCO-ZnPc -liposome	A549	44a
7	Nano-MPs	SPAAC	BCN-Cy5.5 -liposome	U87 and MCF7	44b
8	DCL-AAM	SPAAC	DBCO-Cy5	LS174T	46

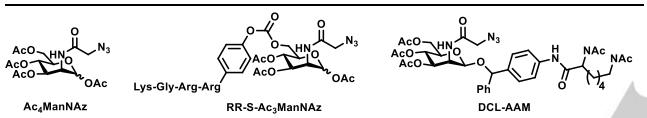

Figure 9. Imaging tumor cell using SPAAC or reactions Staudinger Ligation (SL) *via* a MGE approach.

The reaction was monitored by fluorescence and showed a significantly higher accumulation of DBCO-liposome in mice pre-treated by $Ac_4NanNAz$, thereby proving the efficacy of the *in vivo* SPAAC reaction. The selective introduction of azide groups into cancer cells while sparing healthy cells is also a very challenging task. Several $Ac_4ManNAz$ analogues have been developed (Figure 9, Entries 3-8) to favour intravenous rather than intratumoral injection.[44] For instance, Shim and co-workers developed a cancer cell-specific azide labelling strategy by designing an $Ac_3ManNAz$ derivative (RR-S-$Ac_3ManNAz$) that can be cleaved by cathepsin B overexpressed in tumours to release $Ac_3ManNAz$.[45] They intravenously injected RR-S-$Ac_3ManNAz$ in HT-29-bearing mice, followed by administration of DBCO-Cy5.5. They successfully monitored the fluorescence signal in the tumour with a good signal compared to non-pre-treated mice. Based on the same approach Wang and co-workers exploited two cancer-overexpressed proteases: histone deacetylase and cathepsin L which can selectively deprotected 1-*O*-protected-$Ac_3ManNAz$ (DCL-AAM) to incorporate azides to cancer cells (Figure 9, entry 8).[46] Lee's team synthetized chitosan nanoparticles (CNPs) coated by $Ac_4ManNAz$ to improve the accumulation of $Ac_4ManNAz$ moiety at the tumour site *via* the EPR effect (Figure 9, entry 3).[47] They intravenously injected $Ac_4ManNAz$-CNPs and found a 2-fold higher azide expression on the tumour site than with direct injection of $Ac_4ManNAz$. Cheng's group also adapted MGE to ultrasound-labelling by using $Ac_4ManNAz$-loaded microbubbles (Figure 9, entry 4).[48] They injected these microbubbles in 4T1-bearing-mice and by applying high-amplitude ultrasound released $Ac_4ManNAz$ from them selectively in the tumour. After the injection of DBCO-Cy5, fluorescence monitoring confirmed the efficiency of the process but, unfortunately, this strategy can be used only if the tumour location is well-known.

Based on a different approach, Goun and co-workers reported the development of a bioluminescent glucose-uptake probe for glucose absorption imaging both *in vitro* and *in vivo* (Figure 10).[49]

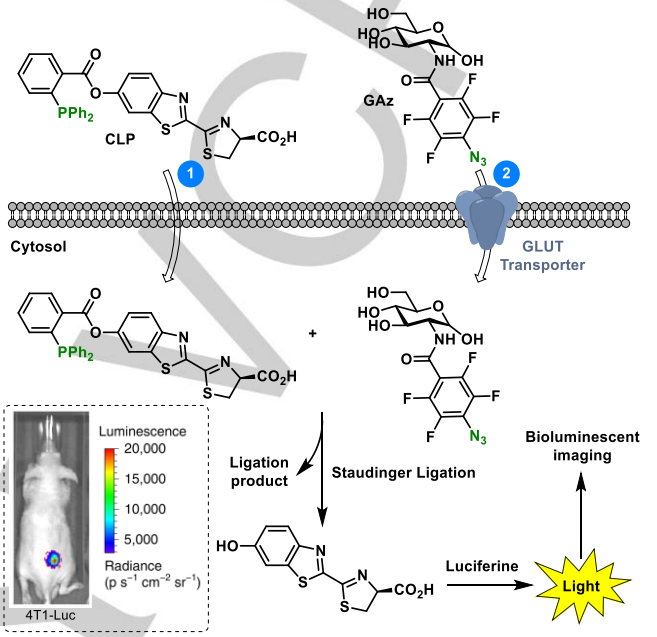

Figure 10. Imaging and quantification of D-glucose uptake in 4T1-Luc-bearing Swiss nu/nu mice using the GAz and CLP. GAz was injected 24 h after CLP.

They designed a triarylphosphine luciferin cleavable ester (CLP) which can accumulate in cells and "decaged" luciferin in presence of a modified-azido-glucose (GAz) *via* SL reaction. The luciferin can further react with Luciferase to produce light, which can be monitored by a specific camera imaging system. They demonstrated the application of their probe by imaging cancer in mice bearing xenograft tumour of 4T1-luc and 4T1-luc GLUT1 knockouts. They observed lower light signal in GLUT1 knockout mice in comparison to 4T1-luc controls. In addition, they proved that this method can be useful to find new GLUT inhibitors *in vivo*. They also brilliantly demonstrated that this approach is comparable to PET imaging in term of sensitivity.

4 *In vivo* biorthogonal chemistry for therapeutic applications

4.1 Biorthogonal systems for selective drug delivery in targeted tissues

The selective activation of non-toxic prodrugs within diseased tissues represents an attractive alternative to standard treatments with the aim to enhance their efficacy, while limiting their adverse effects. In this context, the use of bioorthogonal cleavage or click-and-release reactions for drug decaging at desired locations offers stimulating perspectives for developing more selective therapeutic strategies, since this triggering method is independent of endogenous chemical and biochemical markers (*e.g.* pH, enzymes…). Along the past decade, such approaches have been

investigated *in vivo* through various protocols involving either the preimplantation or the targeting of at least one of the bioorthogonal partners in the tissues of interest. Similar strategies have been also developed for the selective activation of masked probes at specific locations. These studies were mainly conducted to demonstrate that the selected bioorthogonal reactions could occur in animals, thus allowing to envision therapeutic perspectives. The major advances in this field are summarized in the following paragraphs.

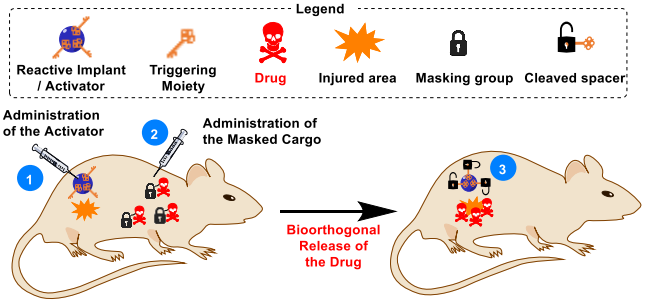

Entry	Animal / output	Activator Galenic	Triggering moiety	Masking group	Drug	Ref.
1	Zebrafish / imaging	Resins (implanted)	Pd^0		Fluorescein	50
2	Mouse / tumor	Nanoparticule (I.V.)	Pd^0		Dox.	51
3	Mouse / tumor	Alginate Hydrogel (implanted)	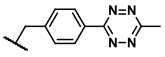	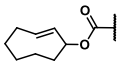	Dox.	52
4	Mouse / infection	Alginate Hydrogel (implanted)	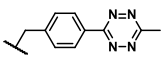	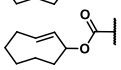	Vancomycin	55
5	Zebrafish / imaging	Polystyrene Beads (implanted)	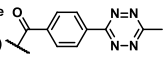	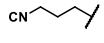	Resorufin	11
6	Zebrafish / heart rate	Polystyrene Beads (implanted)	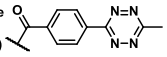	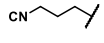	Mexiletin	11
7	Zebrafish / imaging	Small Molecule	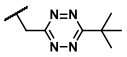	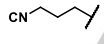	Resorufin / fluorescein	56

Figure 11. Therapeutic strategies designed for the controlled release of drug *via* bioorthogonal cleavage or click-and-release reactions.

By exploring palladium-catalysed depropargylation reactions in biological medium, Bradley and Uniciti-Broceta were the first who highlighted the potential of bioorthogonal cleavage processes in a living organism for biomedical applications (Figure 11, entry 1).[50] In their study, the authors showed that biocompatible Pd^0-resins implanted in the yolk sac of zebrafish embryos displayed catalytic activity enabling the local turn on of a fluorescent probe. This pioneer work was extended few years later by Weissleder and co-workers who reported the activation of an allyloxycarbonyl-protected doxorubicin prodrug within sarcoma HT1080 xenografts in mice (Figure 11, entry 2).[51] This team developed palladium nanoparticles that efficiently accumulated in tumours following their intravenously administration. The subsequent injection of the prodrug induced inhibition of tumour growth with minimal side effects compared to standard therapy, therefore testifying the selective drug decaging in malignant tissues.

With the purpose to design a novel protocol for cancer treatment, Mejia-Oneto and Royzen studied the activation of a TCO-based doxorubicin prodrug by an alginate hydrogel functionalized with Tz moieties (Figure 11, entry 3).[52] It is worth mentioning that polymeric implants bearing bioorthogonal functions had already been studied in mice for *in vivo* imaging.[53],[54] The biomaterial was first injected next to HT-1080 fibrosarcoma xenografts implanted in nude mice. The prodrug was then administered daily for ten days and its therapeutic efficacy was compared to that of the free doxorubicin used at the maximum tolerated dose. In these experiments, the prodrug was found significantly more efficient than the parent drug, inducing total and lasting remission of tumours in 50% of mice. Furthermore, none overt sign of toxicity was observed in the animals treated with the prodrug while mice under therapy with doxorubicin exhibited a strong body weight loss. This study provided evidence that the TCO/Tz click-and-release reaction has proceeded selectively in the vicinity of the tumor mass, thereby resulting in the efficient release of the chemotherapeutic agent.

This concept was also assessed for the therapy of infectious diseases by the same groups (Figure 11, entry 4).[55] In this case, the Tz-modified alginate gel was implanted along with *staphylococcus aureus* bacteria into the thighs of neutropenic mice. The infected animals then received a systemic dose of a TCO-based prodrug of vancomycin, a FDA-approved antibiotic. Quite remarkably, with such a treatment the bacterial infection completely disappeared within 24 hours.

Recently, the Franzini's team described 3-isocyanopropyl substituents as new bioorthogonal masking groups. These latter can be indeed removed by reacting with Tz, thereby leading to the activation of fluorescent probes or the release of drugs (Figure11, entries 5 and 6).[11] Preliminary *in vitro* evaluations showed that this click-and-release reaction was suitable for the decaging of amine-, phenol- and thiol-containing drugs under physiological conditions. *In vivo* assays were then carried out in zebrafish embryos implanted with a Tz-modified polystyrene bead. First, the fishes were exposed to a 3-isocyanopropyl-derivatized resorufin pro-fluorescent probe. In these experiments, the detection of resorufin fluorescence within zebrafishes confirmed the *in vivo* Tz-mediated decaging of the probe. A prodrug of mexiletine, a sodium channel blocker that provokes cardiac arrhythmia and decreases heart rate, was then administered in the animals. This treatment resulted in a slowdown of heart rate in fishes, comparable to that observed with the free drug, hence demonstrating the potential of this approach of drug decaging in living organisms.

As an extension of this work, the same team revealed that tetrazylmethyl (TzMe) protecting groups can be cleaved in the presence of isonitriles to deprotect amine or phenol moieties (Figure 11, entry 7).[56] By combining TzMe derivatives with Tz-responsive 3-isocyanopropyls described above, they demonstrated that two fluorophores can be unmasked by a single bioorthogonal reaction. This double release process was evidenced in zebrafish embryos through the concomitant turn on of two different fluorescent probes. While this study represents a remarkable achievement, the location where the bioorthogonal reaction occurred in the fishes was however not controlled.

Antibody-drug conjugates (ADCs) represent a new class of oncology therapeutics with seven ADCs already approved by the American Food and Drug Administration (FDA) and more than eighty under clinical evaluation.[57] Following their pioneer work on Tz/TCO click-and-release reaction,[8] Robillard and co-workers proposed to use this bioorthogonal process for the selective

cleavage of ADCs.[58],[59] In contrast to the vast majority of ADCs that are internalized inside cancer cells prior to exert their cytotoxic activity, Robillard developed non-internalizing ADCs designed to selectively accumulate on the surface of targeted cancer cells. With such a system, the bioorthogonal reaction leads to the extracellular release of the drug that can subsequently penetrate passively within surrounding cancer cells, even the ones that do not express the targeted surface marker. This concept was first explored in mice bearing TAG72-expressing colon xenografts, with a CC49 antibody linked to doxorubicin *via* TCO (Figure 12, entry 1).[58]

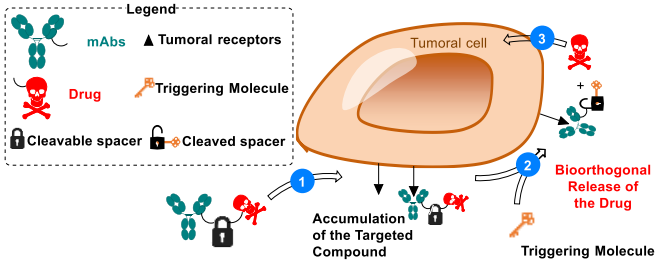

Entry	Targeting Moiety	Bioorthogonaly Cleavable Spacer	Triggering Molecule	Cargo	Ref.
1	Antibody	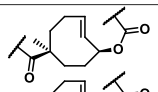		Dox	58
2	Diabody	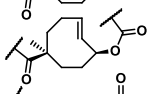		MMAE	59
3	Antibody	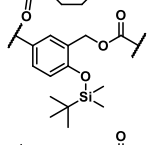	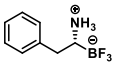	MMAE	60
4	Nanoparticule	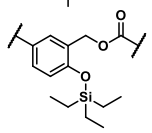	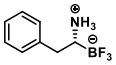	Gasdermine A3	60

Figure 12. Antibody-drug conjugates and nanoparticles designed for the selective delivery of drugs following bioorthogonal activation

After the selective accumulation of ADCs in tumours, the administration of a Tz activator led to the release of doxorubicin in malignant tissues. However, in these experiments, the observed anticancer activity was relatively modest. Indeed, the therapeutic efficacy was impeded by the large size of ADCs that limited their penetration within tumours. Furthermore, a supplementary step devoted to the elimination of non-targeted ADCs was necessary to avoid unselective Tz-mediated release of doxorubicin, therefore increasing the complexity of the therapeutic protocol. To circumvent these drawbacks, Robillard and co-workers developed a diabody-based ADC that exhibits a high tumour uptake and very low retention in healthy tissues (Figure 12, entry 2).[59] In this approach, they also chosen to target the monomethylauristatin E (MMAE) that is far more potent than doxorubicin. As a result, when it was used in combination with a Tz activator, this novel ADC induced a strong anticancer activity in colon and ovarian tumour models in mice. In contrast, the same diabody loaded with the protease-responsive linker employed in the FDA approved Adcetris was not effective for the treatment of such tumours. Thus, this study suggested for the first time that non-internalizing ADCs, bearing bioorthogonal click-and-release systems, could represent a valuable alternative to ADCs already used in clinic for the therapy of some malignancies.

Very recently, Shao and Liu designed an ADC including a fluoride-sensitive cleavable linker that allowed the release of MMAE in the presence of a cancer-imaging probe phenylalanine trifluoroborate ([^{18}F]Phe-BF_3).[60] The originality of this strategy relies on the targeting of each bioorthogonal partners at the tumour site. Indeed, experiences conducted in mice grafted with HER2-positive cancer cells showed the accumulation and retention of both the probe and the trastuzumab-MMAE conjugate, thereby conducting to the selective release of the anticancer drug (Figure 12, entry 3). This result in hands, the authors pursued their investigations using the same linker system to develop bioorthogonal-responsive nanoparticles transporting gasdermin A3 (Figure 12, entry 4). This latter is a pore-forming protein that triggers pyroptosis-induced inflammation, thereby causing antitumor immunity. Proof of principle has been demonstrated in immunocompetent mice with 4T1 mammary xenografts. In these assays, administration of the biorthogonal system led to a total disappearance of the tumour as the consequence of the antitumor immune response.

Our teams also proposed a double tumour targeting strategy using micelles that can be cleaved by a biorthogonal click-and-release SPICC reaction.[61] The micelles were constructed with an iminosydnone amphiphile moiety designed to fragment in the presence of cyclooctynes (Figure 13). In this fashion, the click-and-release process triggers the disassembly of the micelle, hence allowing the controlled delivery of their content. In addition, to avoid the decomposition of untargeted micelles outside the tumour site, Papot and Taran conceived a β-glucuronidase-responsive pro-activator. Due to its high hydrophilicity, this latter cannot penetrate inside the micelles to react with iminosydnone amphiphiles. However, tumour-associated β-glucuronidase can activate the pro-activator to release a hydrophobic cyclooctyne suitable to enter readily micelles and launch their decomposition. This concept was evaluated in mice bearing subcutaneous KB mouth epidermal carcinoma xenografts with micelles loaded with a fluorophore. Selective accumulation of the micelles in tumours was observed 24h following their *i.v.* administration.

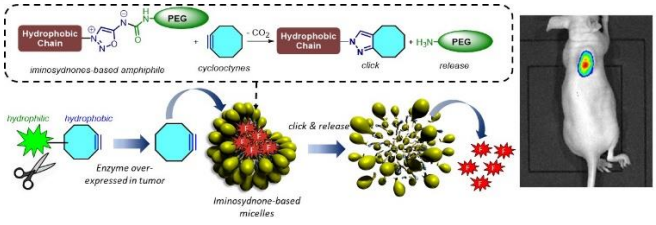

Figure 13. Strategy for double-targeted delivery in tumours. The approach takes advantage of the biorthogonal click-and-release SPICC reaction to deliver the content of nanoparticles.

The subsequent injection of the pro-activator triggered micelles disassembly in malignant tissues demonstrating that the expected sequential enzymatic and bioorthogonal activation process occurred in living mammal.

4.2 Bioorthogonal chemistry for site-specific targeting of nanoparticles

Nanoparticles have emerged as promising tools for various biomedical applications since they can provide improved pharmacokinetics and multifunctionality compared to the majority of small molecules. Within this framework, the efficient targeting

of nanoparticles to the disease site is an important issue that remains to be solved for enhancing their potential as diagnostic and therapeutic agents.

As early as 2012, Kim and co-workers proposed to increase the selectivity of nanoparticles for malignant tissues using bioorthogonal chemistry in combination with MGE.[62] For this purpose, they first carried out intra-tumoral injection of $Ac_4ManNAz$ in mice with A549 lung xenografts. Mice received then fluorescent DBCO-conjugated liposomes that accumulated in tumours as the result of their cooper-free click reaction with the azide groups beforehand generated on the surface of cancer cells. Interestingly, once bound on cell surface, nanoparticles were internalized providing evidence that such a targeting approach could be useful for intracellular delivery.

Two years later, the same group reported a two-step tumour targeting strategy for nanoparticles also based on MGE and click chemistry (Figure 14, entry 1).[47] However, in contrast to their previous study, Kim and co-workers avoided the intra-tumoral administration of $Ac_4ManNAz$ by pre-targeting the azide-modified sugar using glycol chitosan nanoparticles. Intravenous injection of these latter in mice bearing tumours resulted in the generation of azides on the surface of cancer cells due to the selective delivery of $Ac_4ManNAz$ through the EPR effect followed by MGE. In a second time, nanoparticles decorated with BCN and a photosensitizer were administered to the same animals. In this case, the formation of covalent bonds between the nanoparticles and the azides-modified cancer cells allowed to enhance their accumulation in tumours, compared to the targeting based only on the EPR effect. Furthermore, laser irradiation of mice treated with the two-step tumour targeting strategy led to a significant antitumor response correlated excessive local generation of cytotoxic singlet oxygen. This outcome highlighted the potential of this tumour targeting approach for photodynamic therapy.

More recently, the Yao's team investigated a similar targeting protocol for the chemo-photothermal therapy of breast tumours (Figure 14, entry 2).[63] They developed DBCO-functionalized nanocomposites designed for the simultaneous delivery of doxorubicin and a photosensitizer (zinc phthalocyanine). When administered in mice with breast xenografts previously treated by MGE, these nanoparticles showed tumour-specific accumulation, thereby inducing a high tumour-inhibition rate. Moreover, laser irradiation increased the tumour surface temperature to 57°C. On the other hand, such a temperature elevation was not observed in mice that were not pretreated by MGE. Thus, these results clearly demonstrated the advantages brought by the *in vivo* click reaction on the efficiency of photothermal therapy.

In an elegant approach, Zheng, Li and Cai constructed nanoparticles coated with azide-labelled T cell membrane designed to target natural antigen present at the surface of cancer cells by both immune recognition and biorthogonal chemistry (Figure 14, entry 3).[64] Since the sole recognition of T cell receptors is limited by tumours heterogeneity, they proposed this dual targeting strategy as a promising alternative to enhance the accumulation of nanoparticles in malignant tissues. This concept was evaluated in mice bearing Raji tumours pre-treated with Ac_4ManN-BCN. Accumulation in tumours of N_3-labelled nanoparticles loaded with a photosensitizer was 1.5-fold higher than that of the unlabelled ones, 48 h post-injection. Such a result demonstrated unambiguously that the click reaction between the nanoparticles and cancer cells enhanced the efficiency of the targeting. Once again, the increased concentration of nanoparticles within tumours significantly improved the efficacy of photothermal therapy, when mice were submitted to NIR irradiation.

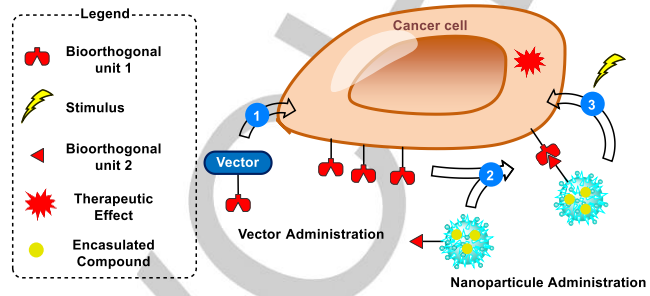

Entry	Bioorthogonal unit 1 (galenic)	Bioorthogonal unit 2	Encapsulated Compound	Tumor Model	Ref.
1	$Ac_4ManNAz$ (nanoparticule)	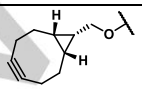	Chlorine e6 (Photosensitizer)	A549	47
2	$Ac_4ManNAz$ (intra-tumoral)	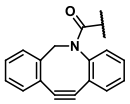	Zinc Phtalocyanine / Doxorubicine	MCF-7	63
3	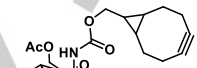 Ac_4ManN-BCN (pretreated cells)	Azide	Indocyanine Green (Photosensitizer)	Raji Cells	64

Figure 14. Strategy combining MGE and click chemistry for site-specific targeting of nanoparticles.

4.3 Pretargeting approach for Radiotherapy

Encouraged by the results observed for imagery purposes using mAb, most pretargeting radioimmunotherapy (PRIT) strategies are based on the same techniques. The bispecific antibody (bsAb) strategy was extensively investigated in PRIT and some of them reached clinical studies. For instance, Kraeber-Bodere *et al*. developed a method involving ^{131}I-hapten with bsAb (directed against CEA antigen) which enabled to detect and treat 70 % of the CEA-expressed tumoral lesions.[65] The biotin streptavidin interaction was also explored in clinical studies using ^{90}Y-biotin as the therapeutic agent[66] but, as previously mentioned, these two techniques have several disadvantages.

In a recent study, SPAAC reaction was evaluated in PRIT using the antibody rituximab (directed against CD20 antigen) in lymphoma cells (Figure 15, entry 1).[67] Au and co-workers functionalized this antibody with DBCO moiety and they synthetized in parallel an ^{90}Y-dendrimer (PAMAM: Poly(amidoamine)) functionalized with azide functions. In this study, they observed a tumour regression in all mice, with 67% of mice becoming tumour free. This success was correlated with the high number of azide functions in the labelled dendrimer which could potentially increase the efficiency of the SPAAC reaction.

Naturally, the Tz/TCO reaction was investigated for PRIT with several radionuclides, such as ^{177}Lu, ^{225}Ac and ^{212}Pb for example, and showed promising results. The first preclinical proof-of-concept of PRIT strategy involving Tz/TCO reaction was successfully performed by Zeglis and co-workers (Figure 15,

entry 2).[68] The authors designed a two-steps strategy with a first *i.v.* injection of 5B1-TCO mAb (directed against CA 19-9) in mice bearing subcutaneous pancreatic tumours followed, 72 h later, by *i.v.* injection of the tetrazine derivative ^{177}Lu-DOTA-PEG$_7$-Tz. They demonstrated a slow-down of tumour growth in treated mice compared to the control group. They also demonstrated a regression of tumour volume for the highest dose (32 MBq). One year later, the same group demonstrated a survival rate of 100 % in subcutaneous colorectal model with their ^{177}Lu-DOTA-PEG$_7$-Tz derivative in pre-treated huA33-TCO mice (Figure 15, entry 3).[69]

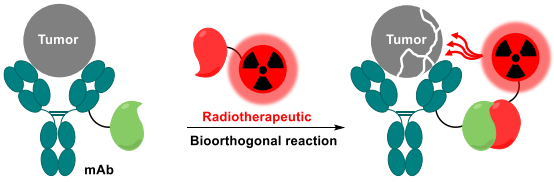

Entry	mAb	Radiotherapeutic	Tumor model	Tumor growth	Ref.
1	CC49-DBCO	PAMAM-N$_3$-^{90}Y	Raji	Regression	67
2	5B1-TCO	Tz-PEG$_7$-DOTA-^{177}Lu	BxPC3	Regression	68
3¤	huA33-TCO	Tz-PEG$_7$-DOTA-^{177}Lu	SW1222	Regression	69
4	35A7-TCO	Tz-PEG$_7$-DOTA-^{177}Lu	A431-CEA-Luc	Slow-down	70
5¤	CC49-TCO	Tz-PEG$_{10}$-DOTA-^{212}Pb	LS174T	Slow-down	33
6	5B1-TCO	Tz-PEG$_7$-DOTA-^{225}Ac	BxPC3	-	71

¤ Survival improvement

Figure 15. Overview of *in vivo* PRIT in mice

In 2019, Rondon and co-workers applied a PRIT method using lutetium-177 in a disseminated model of peritoneal carcinomatosis, for either SPECT imaging or radionuclide-targeted therapy (Figure 15, entry 4).[70] They demonstrated a significant reduction of tumour growth in treated mice compared to the control group that received only saline or 40 MBq of Tz-PEG$_7$-DOTA-^{177}Lu alone.

Compared to *beta*-emitters, *alpha*-emitters can deliver a much more toxic radiation dose in a shorter distance. This characteristic can be evaluated with the linear energy transfer (LET, ratio between the amount of energy emitted and the distance travelled). A higher LET value is advantageous for micro metastases treatment. The first reported Tz-alpha-emitter was labelled with ^{212}Pb ($t_{1/2}$ = 10.6 h, Figure 15, entry 5).[33] The tumour growth rate was reduced using Tz-PEG$_{10}$-DOTA-^{212}Pb in pretreated CC49-TCO mice, compared to mice either treated with a labelled antibody or pretreated with mismatching mAb-TCO. Control experiments showed no reduction of the tumour growth rate when only saline buffer or CC49-TCO were administered. Unfortunately, this study was not further investigated for clinical application since a high kidney uptake was observed (2.5% ID/g 3h p.i.).

Poty and co-worker also demonstrated the ability of ^{225}Ac in PRIT strategy to selectively deliver the radioactivity to the tumour while reducing the haematotoxicity associated with the classical RIT methods (Figure **15** 15, entry 6).[71]

4.4 Bioorthogonal chemistry for the clearance of bioactive molecules

In vivo bioorthogonal chemistry has also been studied to modify 'on demand' the biological activity of drugs. Indeed, long acting and metabolically stable bioactive molecules can produce adverse effects. Consequently, the design of strategies offering the possibility to interrupt the action of some drugs at the desired time is of great interest.

In this context, Krezel and Wagner elaborated a novel approach for neutralizing the activity of an anticoagulant drug in mice (Figure 16, entry 1).[72] For this purpose, they first synthesized an azide-containing analogue of Warfarin, a well-known anti-vitamin K anticoagulant compound, and a hydrophilic clearing agent including a BCN moiety. Then, they demonstrated that the Warfarin analogue exhibited anticoagulant activity in mice. However, administration of the clearing agent led to inactivation of the anticoagulant derivative and induced its plasma elimination *via* renal clearance. This effect was the consequence of the *in vivo* formation of the clicked product that does not possess any anticoagulant activity.

The development of biorthogonal clearing agents was also envisioned for therapeutic applications employing targeted antibodies. This field was pioneered by Robillard *et al.* within the framework of their efforts at designing pretargeting strategies for radiotherapy of solid tumours (Figure 16, entry 2).[31]

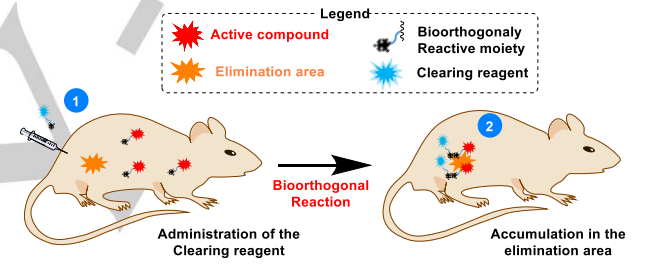

Entry	Target compound	Reactive moiety	Bioothogonal function	Clearing Moiety (Elimination area)	Ref.
1	Warfarin	Azide	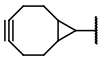	Hydrophilic compound (renal)	72
2	CC49 Antibody	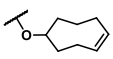	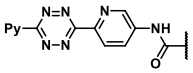	Galactosylated Albumin (liver)	31
3	IgG	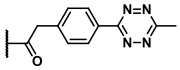	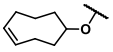	Nanocarrier (liver)	73

Figure 16. Bioorthogonal startegies devoted to the 'on demand' clearance of bioactive molecules.

They investigated a CC49 antibody functionalized by TCO and programmed to react with a radiolabelled Tz selectively in tumour tissues. However, evaluation of this approach in mice failed due to a low tumour-to-blood ratio resulting from the click reaction between the Tz derivatives and untargeted circulating antibodies. To prevent this issue, the authors designed a clearing agent derivatized from albumin including several galactose and Tz moieties. The use of this latter led to a doubling of the Tz tumour uptake and a 125-fold improvement of the tumour-to-blood ratio. Indeed, once in the blood steam, the clearing agent reacted with TCO attached to the CC49 antibody to direct it to the liver while reducing its plasmatic concentration. Along the same line, Simberg and co-workers conceived a set of nanocarriers decorated with bioorthogonal functional groups such as TCO and Tz, with the aim to accelerate the elimination of IgG therapeutic antibodies (Figure 16, entry 3).[73] However, while the click reaction between the two biorthogonal partners occurred *in vivo*,

antibodies were not completely eliminated from the blood, even after multiple injection of the clearing agents. These results pointed out the need of further investigations to optimize antibodies clearance using bioorthogonal chemistry.

5 Summary and Outlook

In less than two decades, bioorthogonal chemistry led to a new paradigm in chemical sciences, showing that living organisms can be used as reaction vessels in which it is possible to control chemical bonds forming and breaking, in spite of the complex conditions prevailing within biological media. While still in its infancy, *in vivo* chemistry offers already great promises to better understanding biological mechanisms in real time as well as for the development of novel biomedical applications. The recent advances in this field highlighted some of the potential issues that have to be taken into account for designing efficient bioorthogonal systems, programmed to operate in live animals. Whereas kinetics of the reactions remains a key factor due to *in vivo* high dilution conditions, biodistribution and circulation time of the reactants play also major roles for the success of chemistry in living organisms. Hence, it is not surprising that many bioorthogonal reactions have been used in combination with delivery systems or targeted strategies. Furthermore, one can expect such combined approaches should develop even more in a near future. These progresses will be of particular interest for therapeutic strategies in which a stringent control of bioorthogonal reactivity will be needed in specific tissues. The discovery of new bioorthogonal reactions will be also necessary to widen the scope of applications of *in vivo* chemistry. To date, it is clear that the number of reactions available remains limited, representing a substantial hurdle for further breakthroughs in this area. Increasing the diversity of biorthogonal tools will probably enable to interact with biological processes in an even more precise manner. Along this line, one could then envision to design multistep synthetic strategies occurring entirely within living organisms.

In summary, the development of bioorthogonal chemistry in animals has already conducted to remarkable achievements letting imagine numerous applications in humans, particularly for diagnosis and therapeutic purposes. However, since this field of research has emerged only few years ago, its potential could be broader than previously anticipated with unexpected applications.

Acknowledgements

This work was funded in part by the French Research National Agency (ANR-19-CE06-0006-01), the Fondation pour la Recherche Médicale (DCM20181039570), the Ligue Nationale contre le Cancer (Comités Vienne and Deux-Sèvres) and the Région Nouvelle Aquitaine (2017-1R30234-00013189).

Keywords: *In vivo* chemistry • chemical biology • bioorthogonal chemistry • click chemistry • pretargeting

[1] H.C. Hang, C. Yu, D. L. Kato, C.R. Bertozzi, *Proc. Natl. Acad. Sci. U. S. A.* **2003**, *100*, 14846–15851.

[2] For review in this field see: a) E. M. Sletten, C. R. Bertozzi, *Angew. Chem. Int. Ed.* **2009**, *48*, 6974–6998; b) R. K. V. Lim, Q. Lin, *Chem. Commun.* **2010**, *46*, 1589–1600; c) C. P. Ramil, Q. Lin, *Chem. Commun.* **2013**, *49*, 11007–11022; d) M. King, A. Wagner, *Bioconjugate Chem.* **2014**, *25*, 825–839; e) L.-H. Qin, W. Hu, Y.-Q. Long, *Tetrahedron Lett.* **2018**, *59*, 2214–2228.

[3] a) A. Borrmann, J. C. M. van Hest, *Chem. Sci.* **2014**, *5*, 2123–2134; b) J. M. Fox, M. S. Robillard, *Curr. Opin. Chem. Biol*. **2014**, 5–7; c) X. Fan, J. Li, P. R. Chen, *Natl Sci Rev*, **2017**, *4*, 300–302; d) H. Y. Yoon, H. Koo, K. Kim, I. C. Kwon, *Biomaterials* **2017**, *132*, 25–36; e) E. Kim, H. Koo. *Chem. Sci.* **2019**, *10*, 7835–7851; f) A. Rondon, F. Degoul, *Bioconjugate Chem.* **2020**, *31*, 159-173.

[4] S. M. van den Bosch, R. Rossin, P. R. Verkerk, W. ten Hoeve, H. M. Janssen, J. Lub, M. S. Robillard, *Nucl. Med. Biol.* **2013**, *40*, 415–423.

[5] D. M. Patterson, L. A. Nazarova, J. A. Prescher, *ACS Chem. Biol.* **2014**, *9*, 592–605.

[6] J Lie, P. R. Chen, *Nat. Chem. Biol*. **2016**, *12*, 129–137.

[7] X. Ji, Z. Pan, B. Yu, L. K. De La Cruz, Y. Zheng, B. Ke, B. Wang, *Chem. Soc. Rev.* **2019**, *48*, 1077-1094.

[8] R. M. Versteegen, R. Rossin, W. ten Hoeve, H. M. Janssen, M. S. Robillard, *Angew. Chem. Int. Ed.* **2013**, *52*, 14112–14116.

[9] a) A. van Onzen, R. M. Versteegen, F. J. M. Hoeben, I. A. W. Filot, R. Rossin, T. Zhu, J. Wu, P. J. Hudson, H. M. Janssen, W. ten Hoeve, M. Robillard, *J. Am. Chem. Soc.* **2020**, *142*, 10955–10963 ; b) M. A.R. de Geus, E. Maurits, A. J. C. Sarris, T. Hansen, M. S. Kloet, K. Kamphorst, W. ten Hoeve, M. S. Robillard, A. Pannwitz, S. A. Bonnet, J. D. C. Codée, D. V. Filippov, H. S. Overkleeft, S. Izaak van Kasteren, *Chem. Eur. J.* **2020**, 10.1002/chem.201905446.

[10] a) S. Bernard, D. Audisio, M. Riomet, S. Bregant, A. Sallustrau, L. Plougastel, E. Decuypere, S. Gabillet, R. A. Kumar, J. Elyian, MN. Trinh, O. Koniev, A. Wagner, S. Kolodych, F.Taran, *Angew. Chem. Int. Ed.* **2017**, *56*, 15612–15616; b) M. Riomet, E. Decuypere, K. Porte, S. Bernard, L. Plougastel, S. Kolodych, D. Audisio, F. Taran, *Chem. Eur. J.* **2018**, *34*, 8535–8541.

[11] a) J. Tu, M. Xu, S. Parvez, R. T. Peterson, R. M. Franzini, *J. Am. Chem. Soc.* **2018**, *140,* 8410−8414; b) 12J. Tu, D. Svatunek, S. Parvez, H. J. Eckvahl, M. Xu, R. T. Peterson, K. N. Houk and R. M. Franzini, *Chem. Sci.* **2020**, *11*, 169–179; c) T. Deb, R. M. Franzini, *Synlett* **2020**, *31*, 938–944.

[12] J. A. Prescher, D. H. Dube, C. R. Bertozzi, *Nature* **2004**, *430*, 873–877.

[13] P. V. Chang, J. A. Prescher, M. J. Hangauer, C. R. Bertozzi, *J. Am. Chem. Soc.* **2007**, *129*, 8400–8401.

[14] K. E. Beatty, J. C. Liu, F. Xie, D. C. Dieterich, E. M. Schuman, Q. Wang, D. A. Tirrell, *Angew. Chem. Int. Ed.* **2006**, *45*, 7364–7367.

[15] M. Sawa, T-L. Hsu, T. Itoh, M. Sugiyama, S. R. Hanson, P. K. Vogt, C-H. Wong, *Proc. Natl. Acad. Sci. U.S.A.* **2006**, *103*, 12371–12376.

[16] a) S. T. Laughlin, J. M. Baskin, S. L. Amacher, C. R. Bertozzi, *Science* **2008**, *320*, 664–667; b) J. M. Baskin, K. W. Dehnert, S. T. Laughlin, L. Amacher, C. R. Bertozzi, *Proc. Natl. Acad. Sci.* **2010**, *107*, 10360–10365.

[17] D. Soriano del Amo, W. Wang, H. Jiang, C. Besanceney, A. C. Yan, M. Levy, Y. Liu, F. L. Marlow, P. Wu, *J. Am. Chem. Soc*. **2010**, *132*, 16893–16899.

[18] H. Jiang, T. Zheng, A. Lopez-Aguilar, L. Feng, F. Kopp, F. L. Marlow, P. Wu, *Bioconjug. Chem*. **2014**, *25*, 698–706.

[19] J. Clavadetscher, S. Hoffmann, A. Lilienkampf, L. Mackay, R. M. Yusop, S. A. Rider, J. J. Mullins, M. Bradley, *Angew. Chem. Int. Ed*. **2016**, *55*, 15662–15666.

[20] P. V. Chang, J. A. Prescher, E. M. Sletten, J. M. Baskin, I. A. Miller, N. J. Agard, A. Lo, C. R. Bertozzi, *Proc. Natl. Acad. Sci.* **2010**, *107*, 1821–1826.

[21] N. Geva-Zatorsky, D. Alvarez, J. E. Hudak, N. C. Reading, D. Erturk-Hasdemir, S. Dasgupta, U. H. von Andrian, D. L. Kasper, *Nat. Med*. **2015**, *21*, 1091–1100.

[22] A. Godinat, H. Min Park, S. C. Miller, K. Cheng, D. Hanahan, L. E. Sanman, M. Bogyo, A. Yu, G. F. Nikitin, A. Stahl, E. A. Dubikovskaya, *ACS Chem. Biol.* **2013**, *8*, 987−999.

[23] D. J. Hnatowich, F. Virzi, M. Rusckowski, *J. Nucl. Med.* **1987**, *28*, 1294−1302.

[24] D. J. Vugts, A. Vervoort, M. S. van Walsum, G. W. M. Visser, M. S. Robillard, R. M. Versteegen, R. C. M. Vulders, J. D. M. Herscheid, G. A. M. S. van Dongen, *Bioconjugate Chem.* **2011**, *22,* 10, 2072–2081.

[25] D.-E. Lee, J. H. Na, S. Lee, C. M. Kang, H.N. Kim, S. J. Han, H. Kim, Y. S. Choe, K-H. Jung, K. C. Lee, K. Choi, I. C. Kwon, S. Y. Jeong, K-H. Lee, K. Kim, *Mol. Pharmaceutics* **2013**, *10*, 2190−2198.

[26] S. M. van den Bosch, R. Rossin, P. Renart Verkerk, W. ten Hoeve, H. M. Janssen, J. Lub, and M. S. Robillard, *Nucl. Med. Biol.* **2013**, *40*, 415−423.

[27] S. B. Lee, H. L. Kim, H. Jeong, S. T. Lim, M. Sohn, and D. W. Kim, *Angew. Chem. Int. Ed.* **2013**, *52*, 10549–10552.

[28] R. Rossin, P. Renart-Verkerk, S. M. van den Bosch, R. C. M. Vulders, I. Verel, J. Lub, M. S. Robillard, *Angew. Chem. Int. Ed.* **2010**, *49*, 3375−3378

[29] N. K. Devaraj, G. M. Thurber, E. J. Keliher, B. Marinelli, R. Weissleder, *PNAS*, **2012**, *109*, 4762-4767.

[30] a) J-P. Meyer, J. L. Houghton, P. Kozlowski, D. Abdel-Atti, T. Reiner, N. V. K. Pillarsetty, W. W. Scholz, B. M. Zeglis, J. S. Lewis, *Bioconjugate Chem*. **2016**, *27*, 298–301; b) A. Rondon, N. Ty, J-B. Bequignat, M. Quintana, A. Briat, T. Witkowski, B. Bouchon, C. Boucheix, E. Miot-Noirault, J-P. Pouget, J-M. Chezal, I. Navarro-Teulon, E. Moreau, F. Degoul, *Sci. Rep.* **2017**, *7*, 14918.

[31] R. Rossin, T. Lappchen, S. M. van den Bosch, R. Laforest, M. S. Robillard, *J. Nucl. Med.* **2013**, *54*, 1989− 1995.

[32] M. F. García, X. Zhang, M. Shah, J. Newton-Northup, P. Cabral, H. Cerecetto, T. Quinn, *Bioorg. Med. Chem.* **2016**, *24*, 1209−1215.

[33] M. A. Shah, X. Zhang, R. Rossin, M.S. Robillard, D. R. Fisher, T. Bueltmann, F. J. M. Hoeben, T. P. Quinn, *Bioconjugate Chem.* **2017**, *28*, 3007−3015.

[34] T. Läppchen, R. Rossin, T. R. van Mourik, G. Gruntz, F. J. M. Hoeben, R. M. Versteegen, H. M. Janssen, J. Lub, M. S. Robillard, *Nucl. Med. Biol.* **2017**, *55*, 19−26.

[35] J.-P. Meyer, K. M. Tully, J. Jackson, T. R. Dilling, T. Reiner, J. S. Lewis, *Bioconjugate Chem.* **2018**, *29*, 538−545.

[36] R. Membreno, O. M. Keinänen, B. E. Cook, K. M. Tully, K. C. Fung, J. S. Lewis, B. M. Zeglis, *Mol. Pharmaceutics* **2019**, *16*, 2259−2263.

[37] S. Hou, J. Choi, M. A. Garcia, Y. X. Kuan-Ju Chen, Y. Chen, Z. K. Jiang, T. R. L. Wu, D. B. Stout, J. S. Tomlinson, H. Wang, K. Chen, H.-R. Tseng, W.-Y. Lin, *ACS Nano,* **2016**, *10*, 1, 1417–1424.

[38] A. Zlitin, M. Yin, N. Janzen, S. Chatterjee, A. Lisok, K. L. Gabrielson, S. Nimmagadda, M. G. Pomper, F. S. Foster, J. F. Valliant, *PLoS ONE*, **2017**, 12(5): e0176958.

[39] A. Rondon, F. Degoul, *Bioconjugate Chem.* **2020**, *31*, 159−173.

[40] M. Richard, C. Truillet, V. L. Tran, H. Liu, K. Porte, D. Audisio, M. Roche, B. Jego, S. Cholet, F. Fenaille, B. Kuhnast, F. Taran, S. Specklin, *Chem. Commun.* **2019**, *55*, 10400−10403.

[41] J. A. Prescher, C. R. Bertozzi, *Cell*, **2006**, *126*, 851−856.

[42] A. A. Neves, H. Stöckmann, R. R. Harmston, H. J. Pryor, I. S. Alam, H. Ireland‐Zecchini, D. Y. Lewis, S. K. Lyons, F. J. Leeper, K. M. Brindle, *FASEB J.* **2011**, *25*, 2528–2537.

[43] H. Koo, S. Lee, J. H. Na, S. H. Kim, S. K. Hahn, K. Choi, I. C. Kwon, S. Y. Jeong, K. Kim, *Angew. Chem. Int. Ed.* **2012**, *51*, 11836–11840.

[44] a) L. Du, H. Qin, T. Ma, T. Zhang, D. Xing, *ACS Nano* **2017**, *11*, 8930–8943; b) S. Lee, S. Jung, H. Koo, J. H. Na, H. Y. Yoon, M. K. Shim, J. Park, J-H. Kim, S. Lee, M. G. Pomper, I. C. Kwon, C-H. Ahn, K. Kim, *Biomaterials* **2017**, *148*, 1–15.

[45] M. K. Shim, H. Y. Yoon, J. H. Ryu, H. Koo, S. Lee, J. H. Park, J. H.; Kim, S. Lee, M. G. Pomper, I. C. Kwon, K. Kim, *Angew. Chem. Int. Ed.* **2016**, 55, 14698–14703.

[46] H. Wang, R. Wang, K. Cai, H. He, Y. Lium J. Yen, Z. Wang, M. Xu, Y. Sun, X. Zhu, Q. Yin, L. Tang, I. T. Dobrucki, L. W. Dobrucki, E. J. Chaney, S. A. Boppart, T. M. Fan, S. Lezmi, X. Chen, L. Yin, J. Cheng, *Nat. Chem. Biol*. **2017**, *13*, 415–424.

[47] S. Lee, H. Koo, J. H. Na, S. Han, H. S. Min, S. J. Lee, S. H. Kim, S. H. Yun, S. Y. Jeong, I. C. Kwon, K. Choi, K. Kim, *ACS Nano* **2014**, *8*, 2048–2063.

[48] H. Wang, M. Gauthier, J. R. Kelly, R. J. Miller, M. Xu, W. D. F. Jr. O'Brien, J. Cheng, *Angew. Chem. Int. Ed.* **2016**, *55*, 5452–5456.

[49] T. Maric, G. Mikhaylov, P. Khodakivskyi, A. Bazhin, R. Sinisi, N. Bonhoure, A. Yevtodiyenko, A. Jones, V. Muhunthan, G. Abdelhady, D. Shackelford, E. Goun, *Nature Methods*, **2019**, *16*, 526–532.

[50] J. T. Weiss, J. C. Dawson, K. G. Macleod, W. Rybski, C. Fraser, C. Torres-Sánchez, E. E. Patton, M. Bradley, N. O. Carragher, A. Unciti-Broceta, *Nat. Commun.* **2014**, *5*, 3277.

[51] M. A. Miller, B. Askevold, H. Mikula, R. H. Kohler, D. Pirovich, R. Weissleder, *Nat. Commun.* **2017**, *8*, 15906.

[52] J. M. Mejia Oneto, I. Khan, L. Seebald, M. Royzen, *ACS Cent. Sci.* **2016**, *2*, 476-482.

[53] N. K. Devaraj, G. M. Thurber, E. J. Keliher, B. Marinelli, R. Weissleder, *PNAS*, **2012**, *109*, 13, 4762-4767.

[54] Y. Brudno, R. M. Desai, B. J. Kwee, N. S. Joshi, M. Aizenberg, D. J. Mooney, *ChemMedChem* **2015**, *10* ,617-620.

[55] M. Czuban, S. Srinivasan,N. A. Yee, E. Agustin, A. Koliszak, E. Miller, I. Khan, I. Quinones, H. Noory, C. Motola, R. Volkmer, M. Di Luca, A. Trampuz, M. Royzen, J. M. Mejia Oneto, *ACS Cent. Sci.* **2018**, *4*, 12, 1624-1632.

[56] J. Tu, D. Svatunek, S. Parvez, H. J. Eckvahl, M. Xu, R. T. Peterson, K. N. Houk, R. M. Franzini, *Chem. Sci.* **2020**, *11*, 169–179.

[57] A. Beck, L. Goetsch, C. Dumontet, N. Corvaïa, *Nat. Rev. Drug Discov.* **2017**, *16*, 315–337.

[58] R. Rossin, S. M. J. van Duijnhoven, W. ten Hoeve, H. M. Janssen, L. H. J. Kleijn, F. J. M. Hoeben, R. M. Versteegen, M. S. Robillard, *Bioconjugate Chem.* **2016**, *27*, 1697−1706.

[59] R. Rossin, R. M. Versteegen, J. Wu, A. Khasanov, H. J. Wessels, E. J. Steenbergen, W. ten Hoeve, H. M. Janssen, A. H.A.M. van Onzen, P. J. Hudson, M. S. Robillard, *Nat. Commun.* **2018**, *9*, 1484.

[60] Q. Wang, Y. Wang, J. Ding, C. Wang, X. Zhou, W. Gao, H. Huang, F. Shao, Z. Liu, *Nature* **2020**, *579*, 421−426.

[61] K. Porte, B. Renoux, E. Péraudeau, J. Clarhaut, B. Eddhif, P. Poinot, E. Gravel, E. Doris, A. Wijkhuisen, D. Audisio, S. Papot, F. Taran. *Angew. Chem. Int. Ed.* **2019**, *58*, 6366−6370.

[62] H. Koo, S. Lee, J. H. Na, S. H. Kim, S. K. Hahn, K. Choi, I. C. Kwon, S. Y. Jeong, K. Kim, *Angew. Chem. Int. Ed.* **2012**, *51*, 11836 -11840.

[63] J. Qiao, F. Tian, Y. Deng, Y. Shang, S. Chen, E. Chang, J. Yao, *Theranostics* **2020**, *10*, 12, 5305−5321.

[64] Y. Han, H. Pan, W. Li, Z. Chen, A. Ma, T. Yin, R. Liang, F. Chen, Y. Ma, Y. Jin, M. Zheng, B. Li, L. Cai, *Adv. Sci.* **2019**, *6*, 1900251.

[65] F. Kraeber-Bodere, C. Rousseau, C. Bodet-Milin, L. Ferrer, A. Faivre-Chauvet, L. Campion, J-P. Vuillez, A. Devillers, C-H. Chang, D. M. Goldenberg, J-F. Chatal, J. Barbet, *J. Nucl. Med.* **2006**, 47, 247−255.

[66] H.B. Breitz, P. L. Weiden, P. L. Beaumier, D. B. Axworthy, C. Seiler, F. M. Su, S. Graves, K. Bryan, J. M. Reno, *J. Nucl. Med.* **2000**, *41*, 1, 131−140.

[67] K. M. Au, A. Tripathy, C. P.-I. Lin, K. Wagner, S. Hong, A. Z. Wang, S. I. Park, *ACS Nano*, **2018**, *12*, 1544−1563.

[68] J. L. Houghton, R. Membreno, D. Abdel-Atti, K. M. Cunanan, S. Carlin, W. W. Scholz, P. B. Zanzonico, J. S. Lewis, B. M. Zeglis, *Mol. Cancer Ther.* **2017**, *16*, 124−133.

[69] R. Membreno, B. E. Cook, K. Fung, J. S. Lewis, B. M. Zeglis, *Mol. Pharmaceutics*, **2018**, *15*, 1729−1734.

[70] A. Rondon, S. Schmitt, A. Briat, N. Ty, L. Maigne, M. Quintana, R. Membreno, B. M. Zeglis, I. Navarro-Teulon, J.-P Pouget, J-M. Chezal, E. Miot-Noirault, E. Moreau, F. Degoul, *Theranostics* **2019**, *9*, 6706−6718.

[71] S. Poty, L. M. Carter, K. Mandleywala, R. Membreno, D. AbdelAtti, A. Ragupathi, W. W. Scholz, B. M. Zeglis, J. S. Lewis, *Clin. Cancer Res.* **2019**, *25*, 868−880.

[72] S. Ursuegui, M. Recher, W. Krężel, A. Wagner, *Nat. Commun.* **2017**, 8, 15242.

[73] W. J. Smith, G. Wang, H. Gaikwad, V. P. Vu, E. Groman, D. W. A. Bourne, D. Simberg, *ACS Nano*. **2018**, *12*, 12523−12532.

Table of Contents

MINIREVIEW

Performing and controlling non-natural chemical reaction inside living organisms is one of the most difficult challenge chemists may have to face. Here we review the recent update in the development of biorthogonal tools useful not only for basic research in chemical biology but also for diagnosis and therapeutic applications.

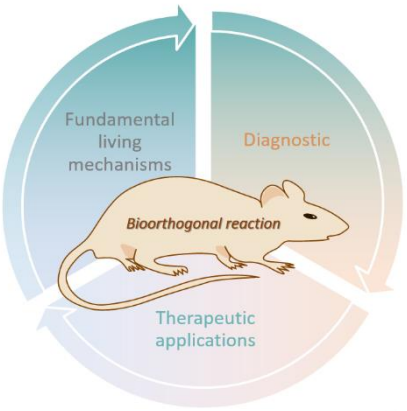

Karine Porte, Maxime Riberaud, Rémi Châtre, Davide Audisio, Sébastien Papot and Frédéric Taran

Page No. – Page No.

Bioorthogonal reactions in animals